JVI Journals.ASM.org

A Novel Activation Mechanism of Avian Influenza Virus H9N2 by Furin

Longping V. Tse,[a,b] Alice M. Hamilton,[a] Tamar Friling,[a] Gary R. Whittaker[a,b]

Department of Microbiology and Immunology, College of Veterinary Medicine, Cornell University, Ithaca, New York, USA[a]; New York Center of Excellence for Influenza Research and Surveillance, University of Rochester Medical Center, Rochester, New York, USA[b]

Avian influenza virus H9N2 is prevalent in waterfowl and has become endemic in poultry in Asia and the Middle East. H9N2 influenza viruses have served as a reservoir of internal genes for other avian influenza viruses that infect humans, and several cases of human infection by H9N2 influenza viruses have indicated its pandemic potential. Fortunately, an extensive surveillance program enables close monitoring of H9N2 influenza viruses worldwide and has generated a large repository of virus sequences and phylogenetic information. Despite the large quantity of sequences in different databases, very little is known about specific virus isolates and their pathogenesis. Here, we characterize a low-pathogenicity avian influenza virus, A/chicken/Israel/810/2001 (H9N2) (Israel810), which is representative of influenza virus strains that have caused severe morbidity and mortality in poultry farms. We show that under certain circumstances the Israel810 hemagglutinin (HA) can be activated by furin, a hallmark of highly pathogenic avian influenza virus. We demonstrate that Israel810 HA can be cleaved in cells with high levels of furin expression and that a mutation that eliminates a glycosylation site in HA_1 allows the Israel810 HA to gain universal cleavage in cell culture. Pseudoparticles generated from Israel810 HA, or the glycosylation mutant, transduce cells efficiently. In contrast, introduction of a polybasic cleavage site into Israel810 HA leads to pseudoviruses that are compromised for transduction. Our data indicate a mechanism for an H9N2 evolutionary pathway that may allow it to gain virulence in a distinct manner from H5 and H7 influenza viruses.

Influenza A virus H9N2 was first isolated in the United States in 1966 in turkeys (1) and was subsequently found to be prevalent among waterfowl and able to spread to poultry worldwide (2–4). H9N2 avian influenza viruses have now become endemic in China and the Middle East (3, 5, 6). The impact of H9N2 influenza virus is not restricted to the poultry industry and avian species; sporadic cases of humans infected by H9N2 have also been reported (7, 8). H9N2 influenza virus is different from H5 and H7 influenza viruses, where some strains are defined as highly pathogenic by the World Organization for Animal Health (OIE) based in part by the presence of multiple basic amino acids in the hemagglutinin (HA) cleavage site (9). All of the isolated strains of H9N2 are of low pathogenicity according to the OIE classification. Despite this, several outbreaks of H9N2 virus infections have caused serious disease, and in some cases a high mortality rate, in domestic poultry farms (10–12). Several known reassortment events of H9N2 with H5N1 mean that H9N2 influenza viruses have the potential to be the donor or acceptor for more virulent influenza viruses (13–15). Furthermore, some H9N2 viruses have similar receptor specificity as human influenza viruses (16). Due to the lack of immunity of the global human population to H9 viruses, these viruses are of some concern from the perspective of pandemic potential for the human population (14, 17).

Influenza virus HA is an important pathogenesis determinant of the virus and plays a crucial role in infection (18). Influenza virus HA needs to be proteolytically cleaved at a defined cleavage site to enable exposure of the fusion peptide during viral entry, which initiates successful infection (19). In most cases, influenza virus HAs have monobasic cleavage sites that contain a single arginine (Arg [R]) at the P1 cleavage position. Such cleavage sites are typically activated by trypsin-like serine proteases (20). This requirement restricts the tropism of influenza viruses to the types of tissues that express the proteases for activation. In some situations, highly pathogenic avian influenza viruses (HPAI) of the H5 and H7 subtypes have gained the ability to systemically infect the host by facilitating the activation of their HAs. HPAI H5 HAs are mutated to have multiple insertions of basic residues (Arg [R] or Lys [K]) at the cleavage site, to gain a polybasic cleavage site, and to make use of more ubiquitously expressed furin-like proteases (20–22).

Furin is a member of the proprotein convertase family that is ubiquitously expressed (23). Although furin is expressed universally, expression levels vary and can be quite low depending on tissue types (24). Under specific conditions, including coinfections with other pathogens, furin expression is elevated (25–27). Substrates of furin are mostly basic in nature, as determined biochemically by fluorescence resonance energy transfer-based peptide assays (28). The minimum sequence requirement of furin is R-X-X-R, which consists of two paired arginine residues at the P1 (cleavage) and P4 position, where X can be any amino acid. However, the presence of a basic residue at P2 enhances furin cleavage markedly (29). Interestingly, the consensus cleavage site of H9N2 influenza virus is predicted to be capable of cleavage by furin, with the sequence of R-S-S-R (serine [Ser or S]). Furthermore, a subset of H9N2 viruses have a mutated cleavage site (R-S-K-R or R-S-R-R) that is predicted to be more optimized for furin cleavage (30). However, several studies have shown that such HA sequences are not efficiently cleaved by furin (31, 32). The inconsis-

Received 12 September 2013 **Accepted** 12 November 2013
Published ahead of print 20 November 2013
Address correspondence to Gary R. Whittaker, grw7@cornell.edu.

doi:10.1128/JVI.02648-13

tency of the biochemical prediction and the actual biological data suggest that other factors may play a role in HA cleavage.

Influenza virus HA is a complex protein, folded in a tertiary structure. In this situation, accessibility of the cleavage site to proteases becomes as important as the primary sequence itself. A notable example of this is the influenza virus A/chicken/Pennsylvania/83 (H5N2) (H5 Penn/83) isolate, which becomes more pathogenic after a single mutation at the bottom of the stalk of HA (33). This mutation eliminates a glycosylation site, which is in very close proximity to the cleavage site. The loss of the bulky sugar moieties is thought to reduce the steric hindrance of the protease to the cleavage site; thus, indirectly increasing the accessibility of the cleavage site. In addition to the polybasic cleavage site, HPAI H7 HAs contain a peptide insert upstream of the HA cleavage site to increase the accessibility of the cleavage site to proteases (22). In other situations (most notably with equine H7N7 viruses), the addition of 11 amino acids adjacent to the cleavage site allowed increased cleavage and fusion activation (34, 35), presumably by repositioning and increasing accessibility of the cleavage site motif. The impact of these types of modifications for H9 influenza virus has not been evaluated.

Here, we use a prototype H9N2 virus (A/chicken/Israel/810/2001 [Israel810]) with an R-S-K-R cleavage site and which is associated with high mortality in poultry. We characterize the possibility of HA activation by furin under different expression conditions and in the context of addition of peptide inserts in the HA cleavage site and removal of glycosylation at the base of the HA stalk. In the present study, we found that the furin expression level is directly proportional to the efficiency of HA cleavage, with implications for viral spread in the host. We also found that the removal of glycosylation site 13, a mutation already present in certain H9N2 field strains, leads to the efficient activation of Israel810 by endogenous furin, showing the potential for a defined constellation of mutations that impact HA activation. Our studies allow better understanding of the virus at the biological level in the context of influenza surveillance data and pandemic preparation.

MATERIALS AND METHODS

Cells, viruses, plasmids, and reagents. 293T/17 (CRL-11268) and MDCK (CCL-34) cells (American Type Culture Collection [ATCC]) were maintained in Dulbecco modified Eagle medium (DMEM) supplemented with 10% heat-inactivated fetal bovine serum (FBS; Gibco), 100 U of penicillin/ml, 10 μg of streptomycin (Cellgro)/ml, and 25 mM HEPES (Cellgro) at 37°C in a 5% CO_2 incubator. DF-1 (CRL-12203), QT-6 (CRL-1708), duck embryo (CCL-141), CGBQ (CCL-169), and LMH (CRL-2117) were maintained according to ATCC recommended conditions. The Israel810 HA gene was synthesized by GeneArt/Life Technologies based on the sequence found in NBCI GenBank (accession number ABS50802). All of the hemagglutinin genes were subcloned into the pEF4 vector (Invitrogen) with the addition of a C9 tag at the C terminus. Point mutations were introduced by QuikChange site-directed mutagenesis kit (Agilent) according to the manufacturer's guidelines. Human furin and chicken furin were cloned from A549 cells and DF-1 cells, respectively, into pCMV-tag1 (Agilent). TPCK-trypsin was obtained from Thermo Scientific.

Cell surface biotinylation and Western blot. 293T cells were grown on poly-D-lysine-treated 24-well plates to 60 to 70% confluence and transfected with total 500 ng of plasmids using Lipofectamine 2000 (Invitrogen) for 18 h. The plates were kept on ice, washed with phosphate-buffered saline (PBS), and incubated with Sulfo-NHS-SS-biotin (250 μg/ml; Sigma) for 30 min. Excess biotin was quenched with glycine (50 mM) for 10 min. Cells were washed with PBS and then lysed by 1× radioimmunoprecipitation assay (RIPA) buffer (Millipore) with Complete protease inhibitor cocktail tablets (Roche) for 10 min. Lysed cells were centrifuged at 18,000 × *g* for 20 min at 4°C, and the supernatant was collected and added to 30 μl of a 50% suspension of streptavidin-agarose beads (Thermo), followed by incubation at 4°C on a rotating shaker for 18 h to pull down biotinylated proteins. The beads were washed three times with RIPA buffer and resuspended in 30 μl of 2× Laemmli sample buffer plus 10% β-mercaptoethanol for Western blotting. HA_0 and HA_2 bands were detected by primary mouse α-C9 (ID4) antibody (BEI Resources, catalog no. NR-3148) and secondary goat α-mouse conjugated to horseradish peroxidase (Thermo).

Quantification of HA cleavage. Western blot images were captured with a Fuji Film LAS-3000 imager. The pixel intensity of individual band was measured using ImageJ, and the relative cleavage efficiencies were calculated by using the following equation: $[(HA_2/(HA_0 + HA_2)] \times 100$.

Tunable expression of ch-furin and h-furin. Chicken furin (ch-furin) and human furin (h-furin) were cloned into pPtunerC from Clontech using the EcoRI and SalI restriction sites. pPtunerC-ch-furin-DD or pPtunerC-h-furin-DD (200 ng) were cotransfected with pEF4-Israel810HA (300 ng) into 293T cells. Shield 1 (Clontech) was added at 6 h posttransfection, and surface biotinylation and Western blotting were performed as described above.

siRNA knockdown assay. 293T cells were grown on poly-D-lysine-treated 24-well plates to 60 to 70% confluence and cotransfected with pEF4-HA plasmids and either ON-TARGETplus nontargeting small interfering RNA (siRNA) or ON-TARGETplus furin siRNA (Thermo) using DharmaFECT Duo (Thermo) for 24 h according to the user manual. Half of the cells were used to perform surface biotinylation to determine HA cleavage. The other half of the cells was harvested for quantitative reverse transcription-PCR (qRT-PCR) to determine the knockdown efficiency.

Quantitative reverse-transcribed qRT-PCR. Approximately 10^6 to 10^7 cells were harvested and spun down at 300 × *g* for 5 min at 4°C. Total RNA from the cell pellet was purified by using an RNeasy minikit (Qiagen) according to the manufacturer's instructions. The RNA concentration was measured by using a UV spectrophotometer Q3000 (Quawell), and the quality was confirmed by using a 260/280-nm ratio, with the ratio values ranging between 2.1 and 2.2. One-step qRT-PCR was performed using QuantiTect SYBR green RT-PCR kit (Qiagen) according to the user manual with 50 ng of RNA input. Human furin primers were acquired from PrimerBank (http://pga.mgh.harvard.edu/primerbank/) (36–38). Primer pairs for h-furin (PrimerBank ID 20336193c1), primers for human glyceraldehyde-3-phosphate dehydrogenase (h-GAPDH), ch-furin, and ch-GAPDH were ordered from QuantiTect primer assays (Qiagen). Reactions were set up on ice on a 96-well plate and run immediately using an Applied Biosystems 7500 Fast Real-Time PCR system. The amplification plot and dissociation curves were analyzed by using 7500 Fast Real-Time PCR software to determine the threshold cycles and the dissociation of each sample. Furin expression level was compared relatively to GAPDH expression and normalized to either 293T cells alone (see Fig. 6C) or no siRNA treatment (see Fig. 4C). The $2^{-\Delta\Delta CT}$ value was calculated as described previously (39).

MLV-based influenza PV transduction assay. To produce murine leukemia virus (MLV)-based pseudoviral particles (PVs), 293T cells were grown on 12-well plates to 50 to 60% confluence and transfected with MLV-gag-pol (350 ng), pTG-luc (500 ng), A/chicken/Korea/MS96/1996 (accession number AAF10404) neuraminidase (NA) (350 ng), HA (350 ng), and furin plasmids (350 ng, specified in each individual experiment) for 48 h using Lipofectamine 2000. Supernatants were harvested and filtered through a 0.45-μm-pore-size filter to remove any cell debris. The filtered supernatants containing PVs were treated with or without trypsin (3 μg/ml) as specified in each experiment for 15 min at 37°C to allow HA activation. After activation, excess trypsin activity was neutralized by addition of a 1:1 ratio of RPMI containing trypsin inhibitor from *Glycine max* (soybean; Sigma-Aldrich). MDCK cells were grown on 24-well plates to 60 to 70% confluence and infected in duplicate by 200 μl of PV-RPMI

A

	Cleavage site P2P1	P1′	Fusion peptide	PiTou-Score
H9 consensus	-PARSSR		GLFGAIAGFIEGGWSGLVAGWYG-	
A/Duck/Hong Kong/W213/1997	.....		.....	3.72
A/Chicken/Hong Kong/G9/1997	.....		.....	3.72
A/Turkey/Wisconsin/1/1966	..V...		.....P.....	-27.00
A/Turkey/Israel/810/2001	....K.		.....P.....	9.14
A/Ostrich/Eshkol/1436/2003	....K.		.....P.....	9.14
A/Quail/Shantou/2061/2000	....R.		.....P.....	8.97
A/Chicken/Israel/786/2001	....N.		.....P.....	-22.27
A/Turkey/Israel/747/2005	....G.		.....P.....	2.84

B

Accession #	Strain Name	Accession #	Strain Name
ABP48866	A/turkey/Avigdor/1209/03	AAZ14979	A/turkey/Avichail/1075/02
AAZ14983.1	A/turkey/Avigdor/1215/03	AAZ15002.1	A/Turkey/Beit HaLevi/1009/02
AAZ14991	A/turkey/Givat Haim/622/02	ABP48870	A/turkey/Brosh/1276/03
AAS48376.1	A/turkey/Givat Haim/810/01	AAZ14980.1	A/turkey/Ein Tzurim/1172/02
AAZ15000.1	A/turkey/Givat Haim/868/02	ABP48864	A/turkey/Hod Ezyon/699/02
AAW29076	A/turkey/Givat Haim/965/02	AAZ14990	A/turkey/Mishmar Hasharon/619/02
AAZ14988	A/turkey/Kfar Vitkin/615/02	ABP48865	A/turkey/Naharia/1013/02
AAZ14989	A/turkey/Kfar Vitkin/616/02	ABP48867	A/turkey/Qevuzat Yavne/1242/03
AAZ14984.1	A/turkey/Kfar Warburg/1224/03	AAZ14981.1	A/turkey/Sapir/1199/02
ABS50798	A/turkey/Israel/619/02	AAW29080	A/ostrich/Eshkol/1436/03
ABS50802	A/turkey/Israel/810/01	ABP48863	A/chicken/Kfar Monash/636/02
ABS50806	A/turkey/Israel/1013/02	AAZ14997	A/chicken/Tel Adashim/812/01
ABS50807	A/turkey/Israel/1209/03	AAZ14999	A/geese/Tel Adashim/830/01
AAZ14992.1	A/turkey/Yedidia/625/02	AAZ14998	A/geese/Tel Adashim/829/01
AAZ14977	A/turkey/Yedidia/911/02		

FIG 1 (A) Multiple sequence alignment of H9 HA. A total of 2,801 sequences obtained from NCBI Influenza Database (http://www.ncbi.nlm.nih.gov/genomes/FLU/FLU.html) were aligned by the MUSCLE alignment program. The HA cleavage site from P6 to P1 and the fusion peptide are shown. H9HA consensus sequence is indicated in boldface; underneath it are representative strains where sequence differences from the consensus H9 HA are indicated by the single-letter amino acid code. Representative strains and their accession numbers are as follows: A/duck/Hong Kong/W213/1997 (BAG72217), A/chicken/Hong Kong/G9/1997 (AAF00701), A/turkey/Wisconsin/1/1966 (BAA14335), A/turkey/Israel/810/2001 (ABS50802), A/ostrich/Eshkol/1436/2003(AAW29080), A/quail/Shantou/2061/2000 (ABM46232), A/chicken/Israel/786/2001 (ABS50800), and A/turkey/Israel/747/2005 (ABS50799). Pitou furin prediction scores of the representative strains, where positive values indicate favorable cleavage by furin with the value proportional to the predicted efficiency of cleavage of a given site, are listed. (B) Summary of strains harbors the same mutation as Israel810. This information was current during the preparation of the manuscript (August 2013).

mixture for 1 h. Then, 500 μl of DMEM plus 2% FBS, HEPES, and penicillin-streptomycin was added to each well, followed by incubation for 48 h for transduction. Cells were lysed by using 1× cell culture lysis reagent (Promega) for 1 h at room temperature on a rocker. The transduction efficiency is measured as relative light units (RLU) using a GloMax-20/20 luminometer (Promega) by mixing 10 μl of lysate and 20 μl of luciferase assay reagent (Promega).

RESULTS

Minimum furin cleavage site in H9 HA. Based on a multiple sequence alignment analysis of a total of 2,801 sequences of H9N2 HA from the Influenza Research Database (FluDB), the consensus sequence of the H9N2 cleavage site was determined to be R-S-S-R (Fig. 1). However, the HA cleavage site of H9 influenza viruses is somewhat variable, particularly at the P2 position, which has predominant substitutions of lysine (K), arginine (R), asparagine (N), and glycine (G). Although R-S-S-R constitutes a minimal furin cleavage site, it is notable that a substantial number of isolates (29/2801 [1%]) have a single Lys (K) substitution at the P2 position of their cleavage site, S321K (based on H3 numbering), that is predicted to be a more optimized substrate for furin (32). Predictive scores for furin cleavage are shown in Fig. 1, based on the Pitou 2.0 furin cleavage prediction algorithm (40). Pitou 2.0 accurately predicts furin cleavage sites by taking into account solvent accessibility and binding strength of residues of protein sequences. A sequence with a negative score is considered to be unfavorable for furin recognition and cleavage, while a positive score is predictive of furin cleavage, with higher values being more predictive.

Israel810 HA (with R-S-K-R cleavage site) is predicted to be cleaved by furin, with the highest score of +9.14 among all of the H9 sequences. In comparison, HPAI A/Chicken/Hong Kong/220/1997 (H5N1) has a score of +13.59 (data not shown). Wisconsin1966 (V-S-S-R) has a negative score, which indicates that it is not able to be cleaved by furin, and the consensus sequence (R-S-S-R) has a score of +3.72. Viruses containing the S321K mutation are clustered in the Middle East and are responsible for several outbreaks in local poultry farms infecting a wide range of avian species (Fig. 1B) (41). The full list of strains containing the 321K substitution, along with their accession numbers, are shown in Fig. 1B. A/Chicken/Israel/810/2003 (H9N2) was selected as a prototype virus representing H9 viruses with the 321K substitution within the Middle East.

Israel810 HA can be cleaved by furin, but cleavage depends on furin expression level. To examine the effect of the 321K substitution in Israel810 HA, a revertant HA (321S) with the cleavage site R-S-S-R was generated by site-directed mutagenesis. This HA was examined by Western blot, along with the wild-type (WT) HA, following cell surface biotinylation of 293T cells. Neither HA type was cleaved by an endogenous protease, predicted to be furin, in 293T cells (Fig. 2A). We hypothesized that endogenous levels of furin may be very low in 293T cells and so not enough for efficient HA cleavage. To test this, plasmids containing HA and either hu-

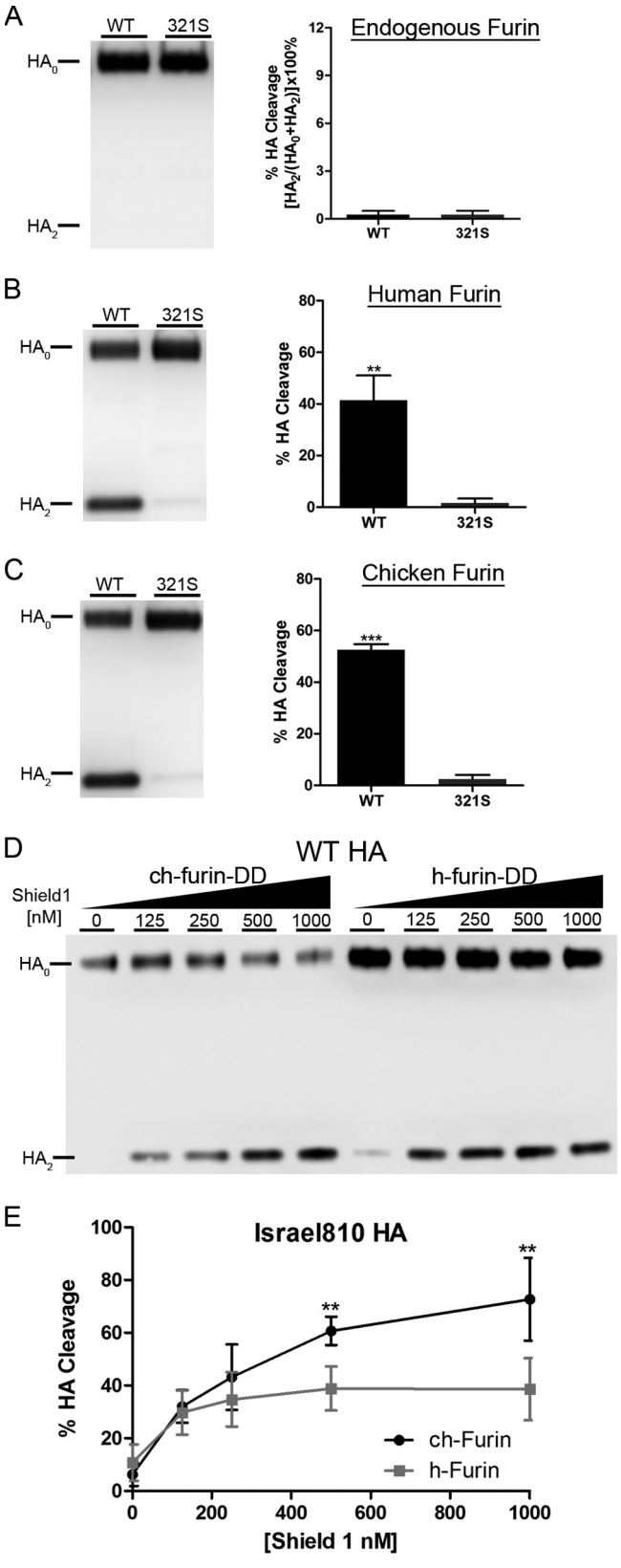

man furin (h-furin) or chicken furin (ch-furin) were cotransfected in 293T cells. Western blot analysis showed that WT HA was able to be efficiently cleaved by either human or chicken furin, whereas the 321S revertant was not (Fig. 2B and C). Israel810 (WT) HA showed 40 and 52% HA cleavage by h-furin and ch-furin, respectively.

Chicken furin has higher processivity than human furin on Israel810 HA. The above data suggested that chicken furin has a higher processivity than human furin in cleaving H9N2 avian influenza virus HA (Fig. 2B and C). To test this observation in a more systematic way, we constructed two tunable expression plasmids for ch-furin and h-furin using the ProteoTuner Shield Systems (Clontech). By fusing the destabilization domain (DD) from the immunophilin FK506-binding protein to the C terminus of each furin, overexpressed furin-DD is degraded by default in proteasomes. Furin-DD can be protected by adding Shield 1, a stabilizing ligand that binds to the DD and prevent it from degradation. Therefore, furin-DD stability can be fine-tuned by the addition of different amounts of Shield 1 into the transfection mix, since the concentration of Shield 1 is directly proportional to the level of overexpressed furin in the cell. Furin-DD and Israel810 (WT) HA were cotransfected into 293T cells supplemented with different concentrations of Shield 1 as described in Materials and Methods. Biotinylation and Western blot analysis showed that HA cleavage is proportional to the concentrations of Shield 1 for both ch-furin and h-furin, where ch-furin showed a higher percentage of HA cleavage than h-furin (Fig. 2D). Quantification of the HA cleavage showed that ch-furin has a higher processivity than h-furin on WT HA and was statistically significant at >500 nM Shield 1 added (Fig. 2E).

Analysis of glycosylation sites close to the cleavage site of H9N2 HA. Since furin-mediated cleavage of Israel810 HA was shown to occur, we examined possible ways for this process to be more efficient. We first assessed likely scenarios for increased cleavage site accessibility via the loss of glycosylation. Three H9N2 isolates have mutations at the bottom of the stalk region of HA_1, which accordingly eliminates the consensus, N-X-S/T motif for N-linked glycosylation (Fig. 3A). According to a homology model of Israel810HA generated by Swiss-Model (42, 43) and Glyprot (http://www.glycosciences.de/modeling/glyprot/php/main.php), and based on the crystal structure of A/Swine/Hong Kong/9/1998 H9N2 (PDB 1JSD), glycan 13 is very close to the HA cleavage site (Fig. 3B). Due to such close proximity, this particular glycosyla-

FIG 2 Cleavage of Israel810HA and Israel810HA-321S by endogenous protease, human furin (h-furin), and chicken furin (ch-furin). (A) Representative Western blot images of HA cleavage by cell surface biotinylation of Israel810HA-WT (WT) and Israel810HA-321S (321S) in 293T cells are shown. The HA_0 and HA_2 bands are labeled. Quantification and statistical analysis results of HA cleavage from the blot are shown on the right. Error bars represent one standard deviation (SD) from at least three independent experiments. The data were analyzed by one-tailed Student *t* test (*, $P < 0.05$; **, $P < 0.01$; ***, $P < 0.005$). (B) Representative Western blots and quantification of WT and 321S HA cleavage by transiently cotransfecting HAs and plasmids expressing h-furin and (C) cf-furin into 293T cells. Error bars represent one SD from at least three independent experiments. Statistical analysis and notations were as described for panel B. (D) Representative Western blot image of surface biotinylation of WT HA cleavage by tunable furin expression system in 293T cells. The concentrations of Shield 1 are indicated at the top of each lane, and HA_0 and HA_2 bands were labeled as described for panel B. (E) Quantification of HA cleavage shown in panel D. The data were analyzed by one-tailed Student *t* test as described for panel B.

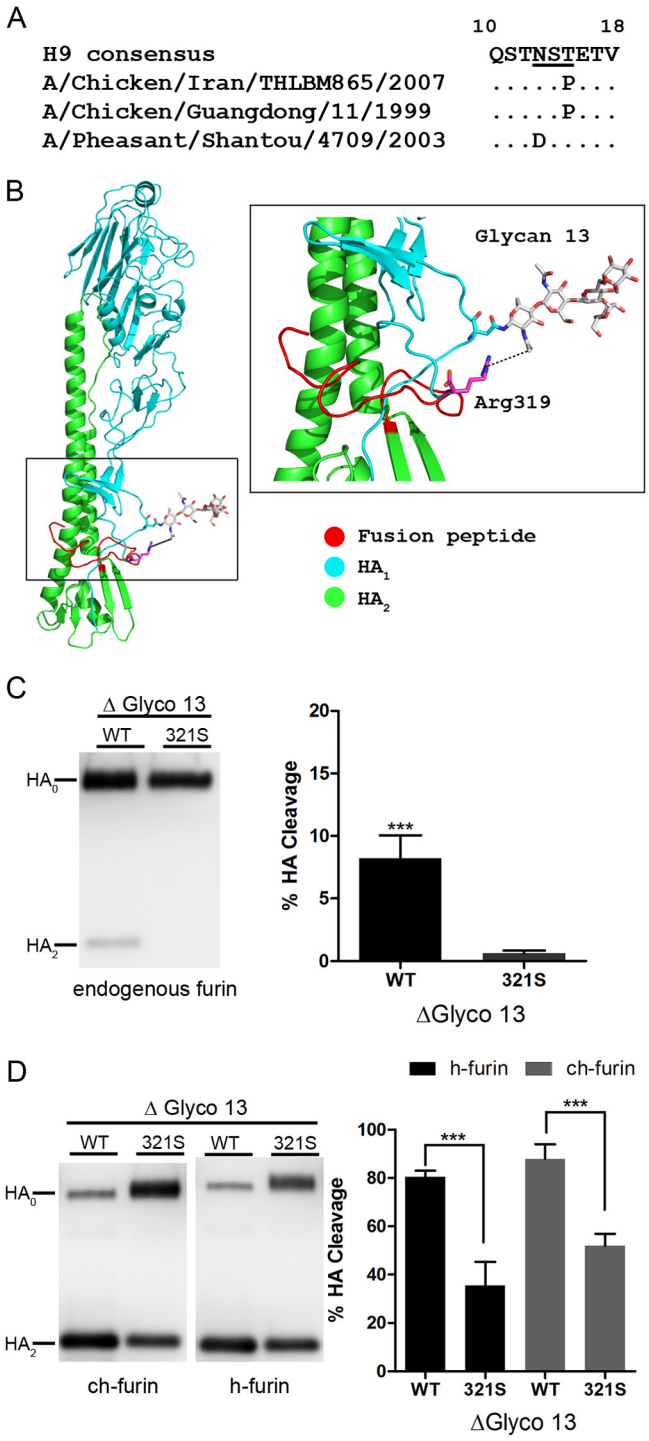

FIG 3 (A) Multiple sequence analysis of H9 HA. Sequence alignment and analysis were performed as in Fig. 1A, amino acids 10 to 18, containing an N-linked glycosylation site (NST), is shown. The H9 HA consensus sequence is indicated in boldface; underneath that are three strains where a single mutation eliminates the potential glycosylation site. Strain names and their accession numbers are as follows: A/chicken/Iran/THLBM865/2007 (ACY25800), A/chicken/Guangdong/11/1999 (ACH95446), and A/pheasant/Shantou/4709/2003 (ABV48004). (B) Homology modeling of Israel810 HA by Swiss-Model based on A/Swine/Hong Kong/9/1998 H9N2 (PDB 1JSD). The bottom of the stem region of a HA monomer is illustrated in diagram form, wherein HA_1 is green, HA_2 is cyan, and the fusion peptide is red. The P4 position of HA cleavage site (Arg319) is magenta, and glycan (Glyco13) is illustrated in stick form in standard CPK colors. The closest distance between Arg322 and Glycan13 was determined by PyMol to be 5.4 Å. (C) HA cleavage of Israel810HA and Israel810HA-321S with a constellation of mutations T15P (ΔGlyco13) by endogenous proteases in 293T cells. Representative Western blot image of HA cleavage by surface biotinylation of Israel810HA-T15P (ΔGlyco13) and Israel810HA-T15P-K321S (321S ΔGlyco13) in 293T cells. HA_0 and HA_2 bands are labeled as indicated. Quantification and statistical analysis results of HA cleavage from the blot are shown on the right. Error bars represent one SD from at least three independent experiments. The data were analyzed by one-tailed Student *t* test (*, $P < 0.05$; **, $P < 0.01$; ***, $P < 0.005$). (D) Representative Western blots and quantification of ΔGlyco13 and 321S ΔGlyco13 cleavage of transiently cotransfecting HAs and plasmids expressing h-furin and ch-furin into 293T cells. Error bars represent one SD from at least three independent experiments. Statistical analysis and notations were same as for Fig. 2A.

tion is likely to affect HA activation by sterically hindering protease accessibility to the HA cleavage site. An equivalent mutation was found on A/chicken/Pennsylvania/83 (H5N2) and was associated with increasing HA activation and thus the pathogenesis of the virus (34, 35). A similar mechanism has also been found on mouse-adapted influenza virus, with an increase in virulence of the virus (44). To further characterize this mutation in the context of H9 HA, we chose to characterize the T15P mutation that was found in two natural isolates: A/chicken/Iran/THLBM865/2007 and A/chicken/Guangdong/11/1999.

HA cleavage of Israel810HA ΔGlyco13 in 293T cells by endogenous protease(s). From the previous data, the Israel810 R-S-K-R cleavage site is not able to be cleaved by endogenous furin (see Fig. 2A). We predicted that the loss of glycosylation site 13 (ΔGlyco13) would likely enhance HA cleavage. To test this hypothesis, two constructs were made and tested after cell surface biotinylation of 293T cells. Western blot analysis showed that "Israel810HA Δ glycosylation 13" (WT ΔGlyco13) can be cleaved by endogenous protease(s) in 293T cells, with ca. 10% of its HA being cleaved which supported our hypothesis. In contrast 321S ΔGlyco13 remains intact in its uncleaved form in 293T cells (Fig. 3C). Cleavage of both ΔGlyco13 HAs is furin dependent, since the overexpression of hu- or ch-furin increases the percentage of HA cleavage. WT ΔGlyco13 showed 80 and 90% HA cleavage by h-furin and ch-furin, respectively, whereas 321S ΔGlyco13 showed 38 and 50% HA cleavage by h-furin and ch-furin, respectively (Fig. 3D). In general, ch-furin showed slightly higher cleavage efficiency than h-furin on all of the HAs tested (Fig. 2B, 2C, and 3D).

Furin is responsible for the cleavage of Israel810 HA. To confirm that the endogenous protease cleaving HA in 293T cells is furin, an siRNA knockdown assay was performed by cotransfecting WT ΔGlyco13 with siRNA targeting h-furin (sih-furin). Western blot data showed that sih-furin decreased the cleavage level from 13% (mock transfected) and 10% (nontargeting siRNA) to 2%, suggesting that furin is the cellular factor that is responsible for HA cleavage in 293T cells (Fig. 4A and B). 321S ΔGlyco13 was used as a negative control of HA cleavage and showed no detectable HA cleavage in all three siRNA treatments (Fig. 4A and B). Control of knockdown was also examined by qRT-PCR. The knockdown efficiency was ca. 50% compared to the mock-transfected control (Fig. 4C). The specificities of qRT-PCR products were monitored in dissociation curves (data not shown), and the PCR products were run on 1% agarose gel for confirmation (Fig. 4C).

HA PVs are activated by endogenous furin. To confirm that

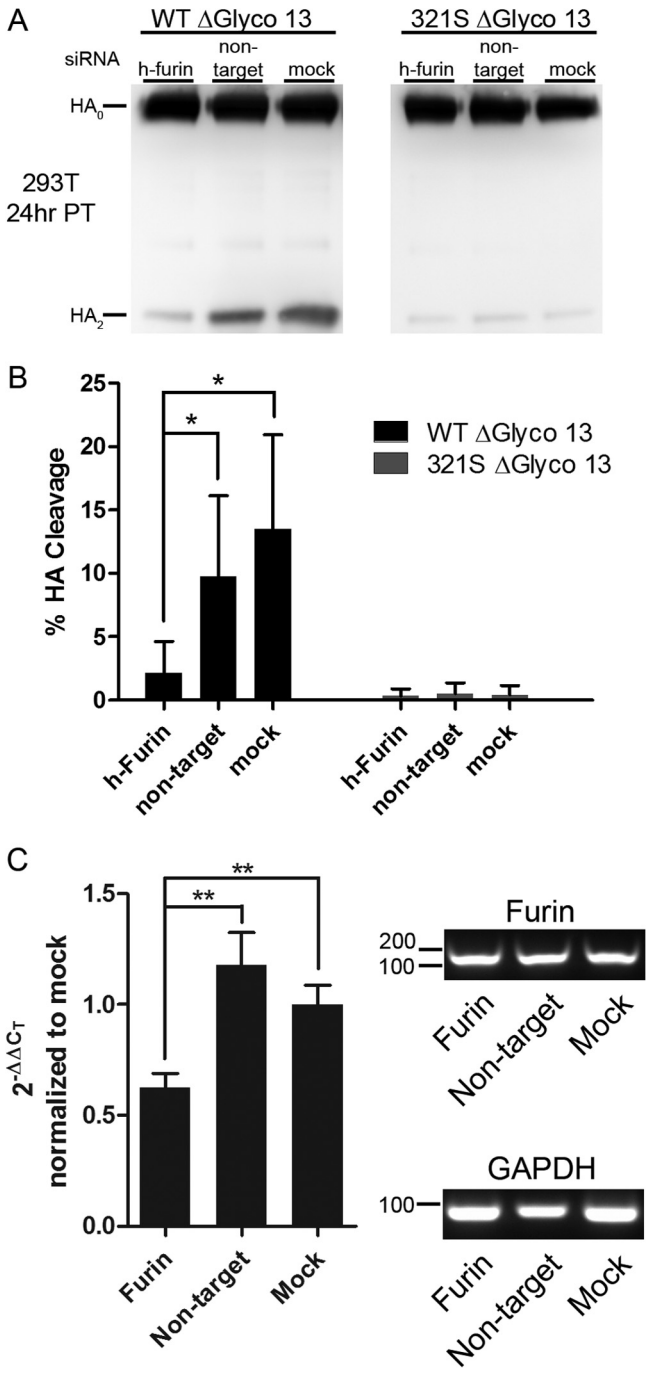

FIG 4 HA cleavage of WT ΔGlyco13 by endogenous furin in 293T cell. (A) Representative Western blot image of HA cleavage by surface biotinylation in 293T cells. Pools of siRNA targeting h-furin (siFurin1-4 [h-furin]), pools of nontargeting siRNA (siNon-target [non-target]), and siRNA resuspending buffer (simock [mock]) were cotransfected with WT ΔGlyco13 into 293T cells as described in Materials and Methods. (B) Quantification and statistical analysis of HA cleavage from Fig. 4A. Error bars represent one SD from at least three independent experiments. (C) Verification of knockdown effect of furin after siRNA treatment. $2^{-\Delta\Delta CT}$ values for h-furin and h-GAPDH were determined by qRT-PCR normalized to mock treatment. On the right, the cDNAs of h-furin and h-GAPDH from qRT-PCR were evaluated on a 1% agarose gel. Error bars represent one SD from three different experiments. Statistical analysis and notation are as described for Fig. 2A.

HA cleavage results in a functional outcome for infection, a PV transduction assay was performed to indirectly quantify HA activation/fusion efficiency. PVs with influenza virus HA and NA on their surfaces were produced in 293T cells and were used to infect MDCK cells. PV infectivity after different treatments is indicated as relative light units (RLU). Trypsin treatment, which activated all of the PVs, was used as an internal control for the total amount of PV being produced. The fold differences between trypsin treatment and no treatment are indicated at the top of each column pair in Fig. 5 and were used as an indirect measurement of HA activation efficiency. All of the trypsin-treated PVs showed a high RLU value (10^7), indicating robust production and transduction of the PVs for all of the HAs tested. The no treatment group revealed a background level (10^3), which indicated no or very little activated particles. The fold difference for trypsin-treated WT ΔGlyco13 is 4,400 times higher than that without trypsin treatment. Although there is a 3-log difference for WT ΔGlyco13, it is slightly lower than the other three groups. The relatively low fold difference of WT ΔGlyco13 HA indicates that it can be activated by endogenous furin slightly better than the other three HAs (Fig. 5A).

HA pseudovirus particles are activated by overexpression of h-furin and ch-furin. To test the functionality of HA activation under overexpression of h-furin and ch-furin, a PV infection assay was performed as described above, except that the PVs were produced in 293T cells transiently transfected with either ch-furin or h-furin. Under both conditions, all four PVs are able to show high transduction level (10^5 to 10^7 RLU) after trypsin treatment, indicating the successful production of PV (Fig. 5B and C). In general, the readings of PVs of the two ΔGlyco13 HAs are ~1 log lower than the WT HA. Of all of the HAs we tested, only 321S cannot be activated by overexpression of h-furin and ch-furin, as reflected by low RLU values (10^3 to 10^4). WT ΔGlyco13 reveals 10^5 RLU regardless of trypsin treatment, indicating all of the PVs are activated before the addition of trypsin. Furthermore, WT HA also shows a very little fold difference between trypsin-treated or non-trypsin- treated conditions with a 5.6-fold difference in h-furin and a 14-fold difference in ch-furin. 321S ΔGlyco13 shows moderate level of activation by h-furin and ch-furin with a 57-fold difference for h-furin and a 510-fold difference for ch-furin.

HA cleavage in avian cell lines correlates with furin expression level. H9N2 virus mainly infect avian species. Therefore, to examine the cleavage of Israel810 HA in cell lines reflecting its natural tropism, we examined the HA activation pattern in different avian cell lines. We performed surface biotinylation using chicken fibroblast (DF-1), quail fibroblast (QT-6), and chicken heptocellular carcinoma (LMH) cells. Similar to 293T cells, all of the cell lines support HA cleavage of WT ΔGlyco13. QT-6, DF-1, and LMH allow 10, 55, and 66% of HA cleavage, respectively, compared to 10% cleavage in 293T cells (Fig. 6A and B). None of the other three HAs were activated in these cell lines (Fig. 6A and B). The mRNA levels of furin relative to GAPDH of these avian cell lines were determined by qRT-PCR and were normalized to 293T cells. The reported $2^{-\Delta\Delta CT}$ values show that furin mRNA levels of DF-1, QT-6, and LMH were 1-, 1.25-, and 1.5-fold higher than those of 293T cells, respectively (Fig. 6C). The cleavage efficiency correlates well with the relative mRNA level of furin in these cell lines.

Substitution of the H9 cleavage site by HPAI H5 and H7 cleavage sites. Another possibility for increased HA cleavage is the insertion of additional basic residues in the cleavage site, as typi-

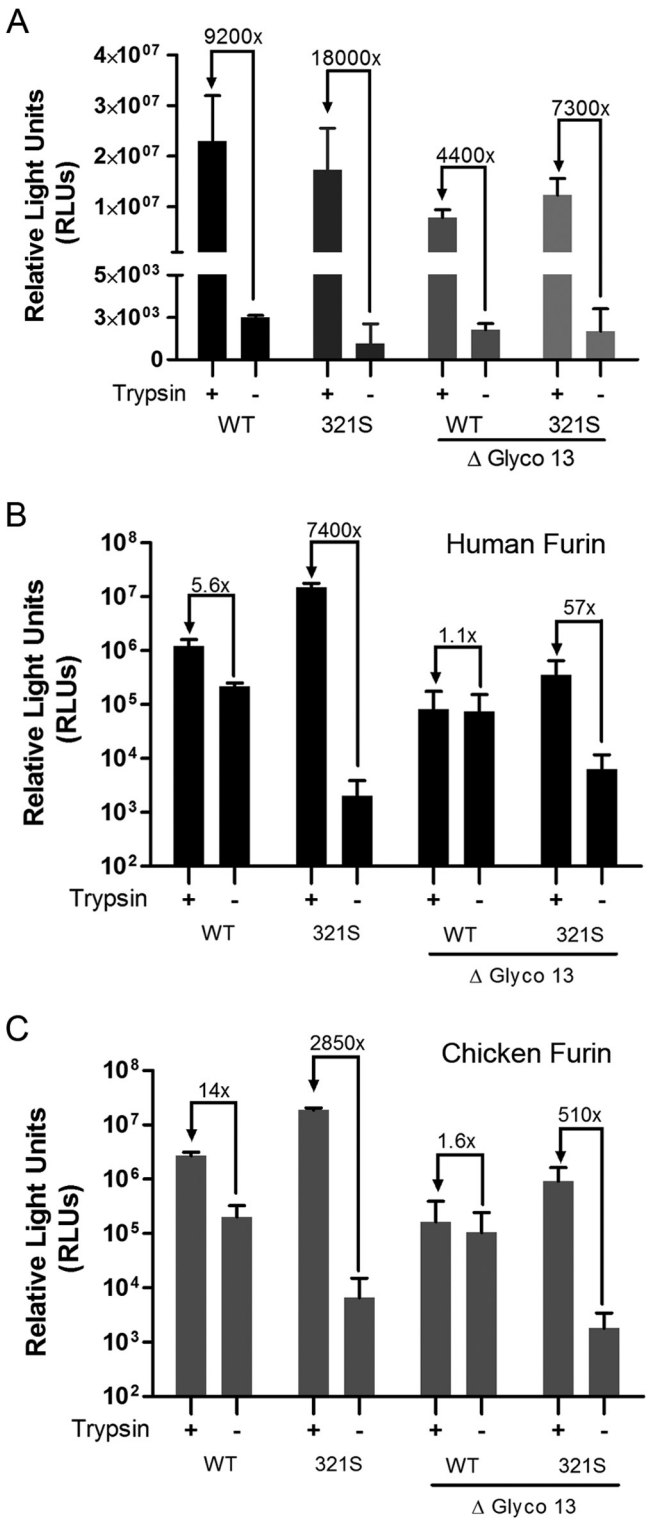

FIG 5 Luciferase-based pseudoviral particle (PV) assay of Israel810HA and mutants produced in cells expressing either endogenous level or overexpressing ch- or h-furin. (A) Quantitative HA-mediated PV transduction assay in MDCK cells. MLV-based PVs with HA and NA on the surface were produced in 293T cells as described in Materials and Methods. Harvested supernatants were either trypsin activated or mock activated before infecting MDCK cells. Infections were performed in duplicates on MDCK cells for 2 days. The cells were lysed, and the relative light units (RLU) were measured after the addition of luciferin. The fold differences between trypsin and nontrypsin treatments are shown at the top of each column pair. Error bars represent one SD of three independent experiments. (B and C) Quantitative HA-mediated PV infection assay in 293T cells expressing h-furin (B) and ch-furin (C). PVs with HA and NA on the surface were produced in 293T cells overexpressing h-furin and ch-furin. Harvested PVs were used to infect MDCK cells in duplicate, and infection was monitored by determining the RLU after addition of luciferin as described in Fig. 5A. Error bars represent one SD of three independent experiments. Statistical analysis was performed as described for Fig. 2A.

fied by H5N1 and H7N7 viruses. According to all the H9 HA sequences in the influenza virus database, H9 HAs have not been reported to contain any polybasic cleavage sites, mimicking H5 or H7 HPAI. To test whether H9 HA is able to accommodate such modification, we substituted the original H9 cleavage site of Israel810 with H5 and H7 HPAI cleavage sites (Fig. 7A). Three constructs were made to mimic the H5N1 HPAI polybasic cleavage site (PB), the 11-amino-acid insertion mimicking HPAI H7N3 isolated in British Columbia in 2004 (45) with a dibasic cleavage site (Insert+DB) or the same insertion with a tribasic cleavage site (Insert+TB) (Fig. 7A).

Cell surface biotinylation and Western blot reveals that PB, Insert+DB and Insert+TB were all able to be cleaved by endogenous furin in 293T cells, in contrast to WT HA shown in earlier experiments (Fig. 7A). The cleavage efficiency varies on different constructs with Insert+TB, with 85% being the highest HA cleavage efficiency. High efficiencies of HA cleavage, 58 and 56%, were also observed for PB and Insert−DB, respectively (Fig. 7B and C). The results of a quantitative PV transduction assay were consistent with those of the biotinylation assays. In general, all constructs were able to incorporate into PV, as shown in trypsin-treated controls. PVs of PB and Insert+TB HA were completely activated with only 2.4- and 2.1-fold differences regardless of trypsin treatment. Insert+DB was activated by furin very well with only a 180-fold difference between treatments. The small differences between treated and untreated samples for all of the HAs indicated a trypsin-independent activation mechanism similar to HPAI (Fig. 7D). Overall, the results of the PV assay corresponded very well to those of the HA cleavage assay and demonstrate that H9 HA is able to accommodate all modifications found in HPAI.

Multiple factors related to the envelope glycoprotein, including stability, expression level, rates of incorporation, receptor binding affinity, and fusion activity, can affect PV transduction efficiency. WT Israel810 HA and ΔGlyco13 HA PVs gave readings of ~10^7 RLU when transducing MDCK cells, indicating similar properties of both HAs at the level of the virion (Fig. 7E). In contrast, all of the PVs with H5 and H7 HPAI-mimicking HAs showed relatively lower readings of approximately 10^4 to 10^5 RLU when transducing MDCK cells. These drops in transduction efficiency suggest that the infectivity of such PVs is compromised (Fig. 7E) and indicate a decrease in viral fitness compared to Israel810 HA and ΔGlyco13 HA.

DISCUSSION

We focused on the cleavage activation of A/chicken/Israel/810/2001, an avian influenza virus with a distinct tribasic cleavage site (R-S-K-R) that is predicted to be cleaved by furin and yet is not defined as highly pathogenic avian influenza virus (HPAI). A/chicken/Israel/810/2001 is representative of viruses with this cleavage site in an epizootic transmission of influenza in the poultry population of Israel between 2001 and 2005 (46). Other H9

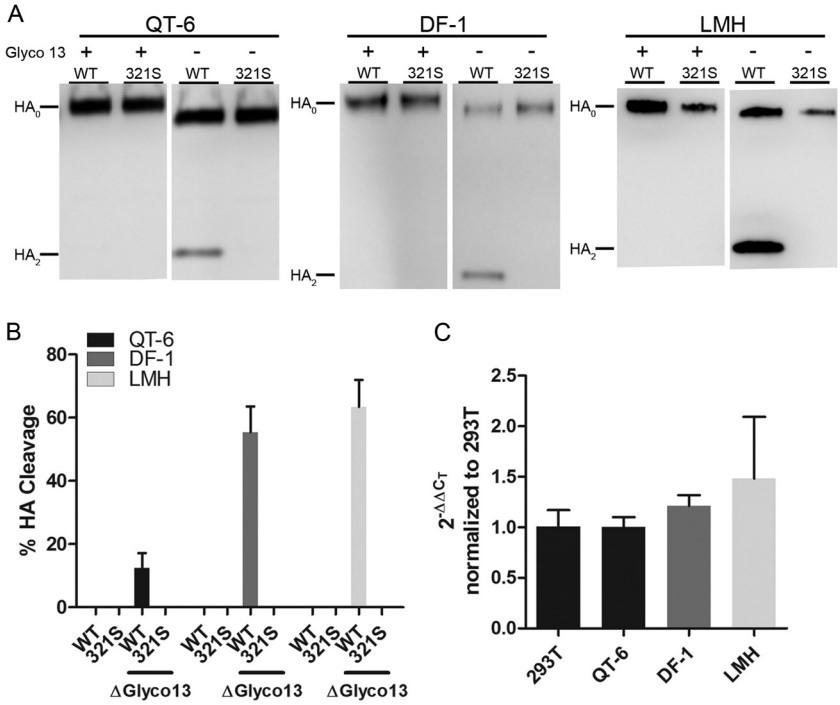

FIG 6 HA cleavage by three different avian cell lines with various levels of furin expression. (A) Representative Western blot image of HA cleavage by surface biotinylation of three different cell lines: quail embryonic fibroblasts (QT-6), chicken embryonic fibroblasts (DF-1), and chicken primary hepatocellular carcinoma epithelial cells (LMH). (B) Quantification and statistical analysis of HA cleavage from Fig. 6A. Error bars represent one SD from at least three independent experiments. Statistical analysis and notations are as described previously for Fig. 2A. (C) qRT-PCR analysis of the relative expression of ch-furin mRNA to ch-GAPDH of the above cell lines. $2^{-\Delta\Delta CT}$ of ch-furin and ch-GAPDH were determined by qRT-PCR and normalized to 293T cells as a reference. Error bars represent one SD from three different experiments starting from RNA extraction. Statistical analysis and notation are described as described above.

viruses with tribasic cleavage sites also meet a similar criteria for furin cleavability without classic HPAI definition (e.g., A/quail/Shantou/2000 with a R-S-R-R cleavage site); however, we chose to study A/chicken/Israel/810/2001 since it is representative of a distinct lineage of H9 viruses with an identical HA cleavage site (29 sequences isolated in Israel over the period from 2001 to 2003). In contrast, quail/Shantou-like viruses with an R-S-R-R cleavage site have only been isolated very sporadically in the field (two isolations in China separated by >10 years, in 2000 and 2011). In addition, an R-S-K-R sequence represents a slightly more optimized furin cleavage motif than R-S-R-R (Pitou scores of 9.14 and 8.97, respectively). We found that the HA of A/chicken/Israel/810/2001 can be cleaved by furin, with cleavage dependent on the Lys (K) residue adjacent to the cleavage site Arg (R). However, the efficiency of HA cleavage was only apparent under high furin expression conditions, with cleavage directly proportional to furin expression level in the cells. Notably, we found that the removal of glycosylation site 13, a mutation already present in certain H9N2 field strains (e.g., A/chicken/Iran/THLBM865/2007), leads to the efficient activation of A/chicken/Israel/810/2001 by endogenous furin, showing the potential for a defined constellation of mutations that impact HA activation. Given the geographic proximity in the sources of these two virus strains in the Middle East, our data highlight the possibility of novel H9 viruses emerging in the field, with increased pathogenicity.

Previous studies have characterized the cleavage activation of H9 viruses with tribasic versus dibasic cleavage sites (i.e., quail/Shantou) and have demonstrated the cleavage of HAs with both cleavage site types by human respiratory proteases (matriptase, TMPRSS2, and HAT) but not by furin (31). It remains to be determined whether an R-S-R-R or R-S-K-R sequence is interchangeable from the perspective of furin cleavage under overexpression conditions and the ability to integrate with glycosylation site changes. The highly similar (although not identical) furin prediction scores for the two sequences indicate that both would behave in an equivalent manner. It is unclear why viruses with a R-S-K-R cleavage site, compared to R-S-R-R, have been found to circulate more widely in nature; this could be due to other changes in HA or other genes or to the poultry production practices in different locations.

Despite the ubiquitous expression of furin, expression levels vary in different cell types, which can be an important determinant for viral infection. As previously shown for infectious bronchitis virus, the level of furin in cells can be a determining factor of their susceptibility to infection (47). Furin levels can also be altered by different triggers. Furin promoter can be upregulated by 3- to 400-fold under hypoxia and iron depletion conditions, respectively (27, 48), which is similar to if not higher than the level of expression produced in our experiments. Also, viral infection, including H5N1 HPAI infection, can induce the expression of a transcription factor, hypoxia-inducible factor 1 (HIF-1), which positively regulates the expression of multiple genes, including furin (49). Furthermore, bacterial infections, such as *Staphylococcus* (50) and *Pseudomonas* (51) infections, which are prevalent in farmed poultry, can also induce HIF-1 and subsequent furin expression. Such induction may allow an unusually high level of

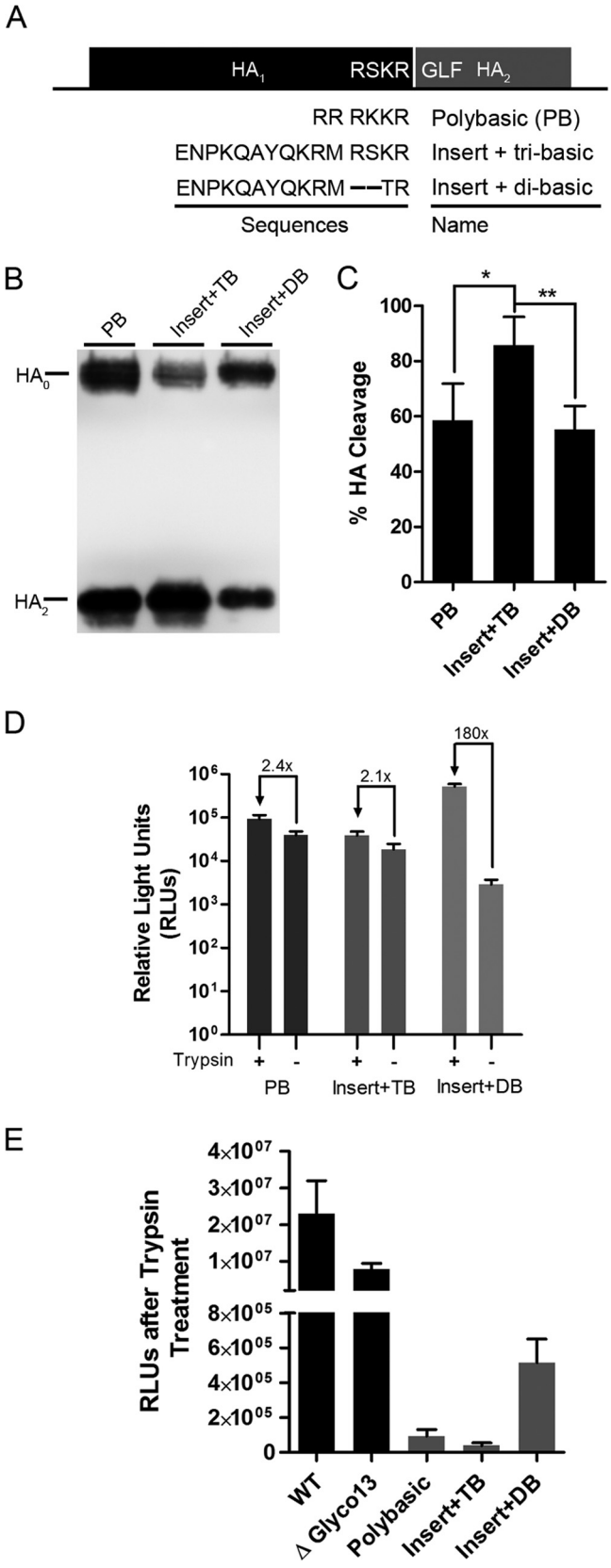

FIG 7 Cleavage and activation of HPAI mimicking H9 mutants by endogenous furin. (A) Illustration of four Israel810HA mutants mimicking HPAI and their cleavage site sequences. Israel810HA WT sequence is illustrated by the two long boxes, and below are the three HPAI mimicking HAs: Israel810HA-H5 polybasic (PB), Israel810HA-H7 insertion plus tribasic site (Insert+TB), and Israel810HA-H7 insertion plus di-basic site (Insert+DB). (B) Representative Western blot of the HPAI-mimicking HA by surface biotinylation. (C) Quantification of HA cleavage in Fig. 7B. Error bars represent one SD from three independent experiments. (D) Quantitative HA-mediated PV transduction assay of the HPAI-mimicking HAs. PVs with the HPAI-mimicking HAs were produced as described in Materials and Methods. Harvested PVs were used to infect MDCK cells, and luciferase activities were used as the indicator of transduction efficiency and HA-mediated membrane fusion. Error bars represent one SD from three independent experiments. Statistical analyses and notations are as described in Fig. 5A. (E) Summary of PV transduction efficiency (expressed as RLU) in MDCK cells after trypsin treatment. Each value was deduced from the corresponding column from Fig. 5A and Fig. 7D and represents the mean of at least three independent PV transduction assay experiments.

furin to activate HA containing R-S-K-R or R-S-S-R cleavage sites that are inert to furin cleavage under normal circumstances. This may also explain the higher mortality and morbidity rate of H9N2 in farmed poultry compared to specific-pathogen-free chickens. The expression level of furin also varies among tissues, with kidneys being one of the tissues with relatively high expression of furin, and may account for the rare event of H9N2 being able to be nephrotropic (52–54).

Avian influenza viruses are grouped into two main categories: low-pathogenicity avian influenza viruses (LPAI) and highly pathogenic avian influenza viruses (HPAI). Transition from LPAI to HPAI is thought to be mediated by a series of mutations within the viral genome. Although some hallmark mutations of HPAI have been characterized, including a polybasic cleavage site for H5 and a cleavage site insertion of H7, the evolution pathway of H9 viruses to become more pathogenic has yet to be fully determined. Over the past decade, several H9N2 outbreaks have shown some intermediate viruses that are certainly more pathogenic than generic LPAI but are below the threshold of being HPAI (10–12, 17). These viruses may serve as intermediates of the H9 evolutionary pathway, allowing the virus to evolve and become more pathogenic. From our data, we show that the constellation of mutations N15T and S321K allows HA to be activated by endogenous furin. Our data and other previous reports suggest that H9 HA is able to accommodate a polybasic site or an 11-amino-acid insertion and still be functionally cleaved by endogenous furin. However, such dramatic changes of H9 HA seem to be deleterious at the level of virion. From our pseudovirus transduction assays, we noticed big drops in PV infectivity (~1 to 2 log in RLU) of these HAs compared to the WT Israel810 HA, which indicates a decrease in viral fitness. This observation may contribute to explaining the puzzling observation that an insertion of a polybasic cleavage site in H9 HA does not convert the virus to HPAI. Our study suggests that a better characterization at the molecular level of influenza virus would help elucidate the broad spectrum of avian influenza virus virulence. For instance, terms such as "moderately pathogenic avian influenza virus" (MPAI) might be used to describe viruses that are more pathogenic than LPAI and show biological features associated with high virulence but do not meet the specific requirements of HPAI set by the OIE. Our studies illustrate that some MPAI, especially H9N2 influenza viruses, require a more thorough examination than just bioinformatics analysis.

HPAI is a generalized phenotype determined by series of complex genotypic changes in influenza virus. HPAI can arise through

different combinations of mutations; therefore, it is predicted that a single mutation would not allow the virus to become HPAI. As shown by other groups, insertion of a polybasic site in H9 HA is not enough to convert the virus from LPAI to HPAI (32, 55). Our results indicate that efficient cleavage activation of an H9 HA by endogenous furin can be achieved by a combination of a tribasic cleavage site (R-S-K-R) and a loss of a glycosylation site at HA_1 residue 13. Each of these features are found individually in nature, and our data show that the combined changes can be tolerated by the HA protein in terms of the folding, stability, and formation of particles. Whether this mutation combination translates into a highly pathogenic virus remains to be tested. Such studies should only be carried out under highly prescribed biosafety conditions and with appropriate administrative oversight. At present, our work is important in the context of influenza pandemic planning.

ACKNOWLEDGMENTS

We thank Jean K. Millet, Xiangjie Sun, and all of the members of the Whittaker lab for helpful discussions. We also thank the Collins lab for helpful suggestions made throughout the study.

These studies were funded by U.S. Department of Health and Human Services contract HHSN266200700008C (NIAID Centers of Excellence for Influenza Research and Surveillance). Work in the author's laboratory is also supported by a research grant from the National Institutes of Health (R01 AI48678).

REFERENCES

1. **Homme PJ, Easterday BC.** 1970. Avian influenza virus infections. I. Characteristics of influenza A/turkey/Wisconsin/1966 virus. Avian Dis. **14:**66–74.
2. **Capua I, Alexander DJ.** 2009. Avian influenza infection in birds: a challenge and opportunity for the poultry veterinarian. Poult. Sci. **88:**842–846. http://dx.doi.org/10.3382/ps.2008-00289.
3. **Guo YJ, Krauss S, Senne DA, Mo IP, Lo KS, Xiong XP, Norwood M, Shortridge KF, Webster RG, Guan Y.** 2000. Characterization of the pathogenicity of members of the newly established H9N2 influenza virus lineages in Asia. Virology **267:**279–288. http://dx.doi.org/10.1006/viro.1999.0115.
4. **Negovetich NJ, Feeroz MM, Jones-Engel L, Walker D, Alam SM, Hasan K, Seiler P, Ferguson A, Friedman K, Barman S, Franks J, Turner J, Krauss S, Webby RJ, Webster RG.** 2011. Live bird markets of Bangladesh: H9N2 viruses and the near absence of highly pathogenic H5N1 influenza. PLoS One **6:**e19311. http://dx.doi.org/10.1371/journal.pone.0019311.
5. **Alexander DJ.** 2003. Report on avian influenza in the eastern hemisphere during 1997-2002. Avian Dis. **47:**792–797. http://dx.doi.org/10.1637/0005-2086-47.s3.792.
6. **Brown IH, Banks J, Manvell RJ, Essen SC, Shell W, Slomka M, Londt B, Alexander DJ.** 2006. Recent epidemiology and ecology of influenza A viruses in avian species in Europe and the Middle East. Dev. Biol. (Basel) **124:**45–50.
7. **Peiris M, Yuen KY, Leung CW, Chan KH, Ip PL, Lai RW, Orr WK, Shortridge KF.** 1999. Human infection with influenza H9N2. Lancet **354:**916–917. http://dx.doi.org/10.1016/S0140-6736(99)03311-5.
8. **Butt KM, Smith GJ, Chen H, Zhang LJ, Leung YH, Xu KM, Lim W, Webster RG, Yuen KY, Peiris JS, Guan Y.** 2005. Human infection with an avian H9N2 influenza A virus in Hong Kong in 2003. J. Clin. Microbiol. **43:**5760–5767. http://dx.doi.org/10.1128/JCM.43.11.5760-5767.2005.
9. **World Organization for Animal Health.** 2008. Manual of diagnostic tests and vaccines for terrestrial animals, 6th ed. World Health Organization/OIE, Geneva, Switzerland.
10. **Lee CW, Song CS, Lee YJ, Mo IP, Garcia M, Suarez DL, Kim SJ.** 2000. Sequence analysis of the hemagglutinin gene of H9N2 Korean avian influenza viruses and assessment of the pathogenic potential of isolate MS96. Avian Dis. **44:**527–535. http://dx.doi.org/10.2307/1593091.
11. **Banet-Noach C, Perk S, Simanov L, Grebenyuk N, Rozenblut E, Pokamunski S, Pirak M, Tendler Y, Panshin A.** 2007. H9N2 influenza viruses from Israeli poultry: a five-year outbreak. Avian Dis. **51:**290–296. http://dx.doi.org/10.1637/7590-040206R1.1.
12. **Nili H, Asasi K.** 2003. Avian influenza (H9N2) outbreak in Iran. Avian Dis. **47:**828–831. http://dx.doi.org/10.1637/0005-2086-47.s3.828.
13. **Xu KM, Li KS, Smith GJ, Li JW, Tai H, Zhang JX, Webster RG, Peiris JS, Chen H, Guan Y.** 2007. Evolution and molecular epidemiology of H9N2 influenza A viruses from quail in southern China, 2000 to 2005. J. Virol. **81:**2635–2645. http://dx.doi.org/10.1128/JVI.02316-06.
14. **Lin YP, Shaw M, Gregory V, Cameron K, Lim W, Klimov A, Subbarao K, Guan Y, Krauss S, Shortridge K, Webster R, Cox N, Hay A.** 2000. Avian-to-human transmission of H9N2 subtype influenza A viruses: relationship between H9N2 and H5N1 human isolates. Proc. Natl. Acad. Sci. U. S. A. **97:**9654–9658. http://dx.doi.org/10.1073/pnas.160270697.
15. **Zhang P, Tang Y, Liu X, Liu W, Zhang X, Liu H, Peng D, Gao S, Wu Y, Zhang L, Lu S.** 2009. A novel genotype H9N2 influenza virus possessing human H5N1 internal genomes has been circulating in poultry in eastern China since 1998. J. Virol. **83:**8428–8438. http://dx.doi.org/10.1128/JVI.00659-09.
16. **Matrosovich MN, Krauss S, Webster RG.** 2001. H9N2 influenza A viruses from poultry in Asia have human virus-like receptor specificity. Virology **281:**156–162. http://dx.doi.org/10.1006/viro.2000.0799.
17. **Abdel-Moneim AS, Afifi MA, El-Kady MF.** 2012. Isolation and mutation trend analysis of influenza A virus subtype H9N2 in Egypt. Virol. J. **9:**173. http://dx.doi.org/10.1186/1743-422X-9-173.
18. **Skehel JJ, Wiley DC.** 2000. Receptor binding and membrane fusion in virus entry: the influenza hemagglutinin. Annu. Rev. Biochem. **69:**531–569. http://dx.doi.org/10.1146/annurev.biochem.69.1.531.
19. **Steinhauer DA.** 1999. Role of hemagglutinin cleavage for the pathogenicity of influenza virus. Virology **258:**1–20. http://dx.doi.org/10.1006/viro.1999.9716.
20. **Klenk H-D, Garten W.** 1994. Activation cleavage of viral spike proteins by host proteases, p 241–280. *In* Wimmer E (ed), Cellular receptors for animal viruses. Cold Spring Harbor Laboratory Press, Cold Spring Harbor, NY.
21. **Kawaoka Y, Webster RG.** 1988. Sequence requirements for cleavage activation of influenza virus hemagglutinin expressed in mammalian cells. Proc. Natl. Acad. Sci. U. S. A. **85:**324–328. http://dx.doi.org/10.1073/pnas.85.2.324.
22. **Lee CW, Lee YJ, Senne DA, Suarez DL.** 2006. Pathogenic potential of North American H7N2 avian influenza virus: a mutagenesis study using reverse genetics. Virology **353:**388–395. http://dx.doi.org/10.1016/j.virol.2006.06.003.
23. **Seidah NG, Mayer G, Zaid A, Rousselet E, Nassoury N, Poirier S, Essalmani R, Prat A.** 2008. The activation and physiological functions of the proprotein convertases. Int. J. Biochem. Cell Biol. **40:**1111–1125. http://dx.doi.org/10.1016/j.biocel.2008.01.030.
24. **Shapiro J, Sciaky N, Lee J, Bosshart H, Angeletti RH, Bonifacino JS.** 1997. Localization of endogenous furin in cultured cell lines. J. Histochem. Cytochem. **45:**3–12. http://dx.doi.org/10.1177/002215549704500102.
25. **Su AI, Wiltshire T, Batalov S, Lapp H, Ching KA, Block D, Zhang J, Soden R, Hayakawa M, Kreiman G, Cooke MP, Walker JR, Hogenesch JB.** 2004. A gene atlas of the mouse and human protein-encoding transcriptomes. Proc. Natl. Acad. Sci. U. S. A. **101:**6062–6067. http://dx.doi.org/10.1073/pnas.0400782101.
26. **Werth N, Beerlage C, Rosenberger C, Yazdi AS, Edelmann M, Amr A, Bernhardt W, von Eiff C, Becker K, Schafer A, Peschel A, Kempf VA.** 2010. Activation of hypoxia inducible factor 1 is a general phenomenon in infections with human pathogens. PLoS One **5:**e11576. http://dx.doi.org/10.1371/journal.pone.0011576.
27. **McMahon S, Grondin F, McDonald PP, Richard DE, Dubois CM.** 2005. Hypoxia-enhanced expression of the proprotein convertase furin is mediated by hypoxia-inducible factor 1: impact on the bioactivation of proproteins. J. Biol. Chem. **280:**6561–6569. http://dx.doi.org/10.1074/jbc.M413248200.
28. **Izidoro MA, Gouvea IE, Santos JA, Assis DM, Oliveira V, Judice WA, Juliano MA, Lindberg I, Juliano L.** 2009. A study of human furin specificity using synthetic peptides derived from natural substrates, and effects of potassium ions. Arch. Biochem. Biophys. **487:**105–114. http://dx.doi.org/10.1016/j.abb.2009.05.013.
29. **Thomas G.** 2002. Furin at the cutting edge: from protein traffic to embryogenesis and disease. Nat. Rev. Mol. Cell. Biol. **3:**753–766. http://dx.doi.org/10.1038/nrm934.
30. **Krysan DJ, Rockwell NC, Fuller RS.** 1999. Quantitative characterization of furin specificity. Energetics of substrate discrimination using an internally consistent set of hexapeptidyl methylcoumarinamides. J. Biol. Chem. **274:**23229–23234.
31. **Baron J, Tarnow C, Mayoli-Nussle D, Schilling E, Meyer D, Hammami**

M, Schwalm F, Steinmetzer T, Guan Y, Garten W, Klenk HD, Bottcher-Friebertshauser E. 2012. Matriptase, HAT, and TMPRSS2 activate the hemagglutinin of H9N2 influenza A viruses. J. Virol. **87:**1811–1820. http://dx.doi.org/10.1128/JVI.02320-12.

32. **Gohrbandt S, Veits J, Breithaupt A, Hundt J, Teifke JP, Stech O, Mettenleiter TC, Stech J.** 2011. H9 avian influenza reassortant with engineered polybasic cleavage site displays a highly pathogenic phenotype in chicken. J. Gen. Virol. **92:**1843–1853. http://dx.doi.org/10.1099/vir.0.031591-0.
33. **Kawaoka Y, Naeve CW, Webster RG.** 1984. Is virulence of H5N2 influenza viruses in chickens associated with loss of carbohydrate from the hemagglutinin? Virology **139:**303–316. http://dx.doi.org/10.1016/0042-6822(84)90376-3.
34. **Gibson CA, Daniels RS, Oxford JS, McCauley JW.** 1992. Sequence analysis of the equine H7 influenza virus hemagglutinin gene. Virus Res. **22:**93–106. http://dx.doi.org/10.1016/0168-1702(92)90037-A.
35. **Hamilton BS, Sun X, Chung C, Whittaker GR.** 2012. Acquisition of a novel eleven amino acid insertion directly N-terminal to a tetrabasic cleavage site confers intracellular cleavage of an H7N7 influenza virus hemagglutinin. Virology **434:**88–95. http://dx.doi.org/10.1016/j.virol.2012.09.004.
36. **Spandidos A, Wang X, Wang H, Seed B.** 2010. PrimerBank: a resource of human and mouse PCR primer pairs for gene expression detection and quantification. Nucleic Acids Res. **38:**D792–D799. http://dx.doi.org/10.1093/nar/gkp1005.
37. **Spandidos A, Wang X, Wang H, Dragnev S, Thurber T, Seed B.** 2008. A comprehensive collection of experimentally validated primers for polymerase chain reaction quantitation of murine transcript abundance. BMC Genomics **9:**633. http://dx.doi.org/10.1186/1471-2164-9-633.
38. **Wang X, Seed B.** 2003. A PCR primer bank for quantitative gene expression analysis. Nucleic Acids Res. **31:**e154. http://dx.doi.org/10.1093/nar/gng154.
39. **Livak KJ, Schmittgen TD.** 2001. Analysis of relative gene expression data using real-time quantitative PCR and the $2^{-\Delta\Delta CT}$ method. Methods **25:**402–408. http://dx.doi.org/10.1006/meth.2001.1262.
40. **Tian S, Huajun W, Wu J.** 2012. Computational prediction of furin cleavage sites by a hybrid method and understanding mechanism underlying diseases. Sci. Rep. **2:**261.
41. **Golender N, Panshin A, Banet-Noach C, Nagar S, Pokamunski S, Pirak M, Tendler Y, Davidson I, Garcia M, Perk S.** 2008. Genetic characterization of avian influenza viruses isolated in Israel during 2000-2006. Virus Genes **37:**289–297. http://dx.doi.org/10.1007/s11262-008-0272-7.
42. **Arnold K, Bordoli L, Kopp J, Schwede T.** 2006. The SWISS-MODEL workspace: a web-based environment for protein structure homology modeling. Bioinformatics **22:**195–201. http://dx.doi.org/10.1093/bioinformatics/bti770.
43. **Kiefer F, Arnold K, Kunzli M, Bordoli L, Schwede T.** 2009. The SWISS-MODEL Repository and associated resources. Nucleic Acids Res. **37:**D387–D392. http://dx.doi.org/10.1093/nar/gkn750.
44. **Brown EG, Liu H, Kit LC, Baird S, Nesrallah M.** 2001. Pattern of mutation in the genome of influenza A virus on adaptation to increased virulence in the mouse lung: identification of functional themes. Proc. Natl. Acad. Sci. U. S. A. **98:**6883–6888. http://dx.doi.org/10.1073/pnas.111165798.
45. **Pasick J, Handel K, Robinson J, Copps J, Ridd D, Hills K, Kehler H, Cottam-Birt C, Neufeld J, Berhane Y, Czub S.** 2005. Intersegmental recombination between the haemagglutinin and matrix genes was responsible for the emergence of a highly pathogenic H7N3 avian influenza virus in British Columbia. J. Gen. Virol. **86:**727–731. http://dx.doi.org/10.1099/vir.0.80478-0.
46. **Perk S, Panshin A, Shihmanter E, Gissin I, Pokamunski S, Pirak M, Lipkind M.** 2006. Ecology and molecular epidemiology of H9N2 avian influenza viruses isolated in Israel during 2000-2004 epizootic. Dev. Biol. (Basel) **124:**201–209.
47. **Tay FP, Huang M, Wang L, Yamada Y, Liu DX.** 2012. Characterization of cellular furin content as a potential factor determining the susceptibility of cultured human and animal cells to coronavirus infectious bronchitis virus infection. Virology **433:**421–430. http://dx.doi.org/10.1016/j.virol.2012.08.037.
48. **Silvestri L, Pagani A, Camaschella C.** 2008. Furin-mediated release of soluble hemojuvelin: a new link between hypoxia and iron homeostasis. Blood **111:**924–931. http://dx.doi.org/10.1182/blood-2007-07-100677.
49. **Tolnay AE, Baskin CR, Tumpey TM, Sabourin PJ, Sabourin CL, Long JP, Pyles JA, Albrecht RA, Garcia-Sastre A, Katze MG, Bielefeldt-Ohmann H.** 2010. Extrapulmonary tissue responses in cynomolgus macaques (*Macaca fascicularis*) infected with highly pathogenic avian influenza A (H5N1) virus. Arch. Virol. **155:**905–914. http://dx.doi.org/10.1007/s00705-010-0662-8.
50. **Beerlage C, Greb J, Kretschmer D, Assaggaf M, Trackman PC, Hansmann ML, Bonin M, Eble JA, Peschel A, Brune B, Kempf VA.** 2013. Hypoxia-inducible factor 1-regulated lysyl oxidase is involved in *Staphylococcus aureus* abscess formation. Infect. Immun. **81:**2562–2573. http://dx.doi.org/10.1128/IAI.00302-13.
51. **Kirienko NV, Kirienko DR, Larkins-Ford J, Wahlby C, Ruvkun G, Ausubel FM.** 2013. *Pseudomonas aeruginosa* disrupts *Caenorhabditis elegans* iron homeostasis, causing a hypoxic response and death. Cell Host Microbe **13:**406–416. http://dx.doi.org/10.1016/j.chom.2013.03.003.
52. **Mosleh N, Dadras H, Mohammadi A.** 2009. Molecular quantitation of H9N2 avian influenza virus in various organs of broiler chickens using TaqMan real-time PCR. J. Mol. Genet. Med. **3:**152–157.
53. **Hadipour MM, Farjadian SH, Azad F, Kamravan M, Dehghan A.** 2011. Nephropathogenicity of H9N2 avian influenza virus in commercial broiler chickens following intratracheal inoculation. J. Anim. Vet. Adv. **10:**1706–1710. http://dx.doi.org/10.3923/javaa.2011.1706.1710.
54. **Pazani J, Marandi MV, Ashrafihelan J, Marjanmehr SH, Ghods F.** 2008. Pathological studies of A/chicken/Tehran/ZMT-173/99 (H9N2) influenza virus in commercial broiler chickens of Iran. Int. J. Poult. Sci. **5:**502–510.
55. **Soda K, Asakura S, Okamatsu M, Sakoda Y, Kida H.** 2011. H9N2 influenza virus acquires intravenous pathogenicity on the introduction of a pair of di-basic amino acid residues at the cleavage site of the hemagglutinin and consecutive passages in chickens. Virol. J. **8:**64. http://dx.doi.org/10.1186/1743-422X-8-64.